

RESEARCH

Open Access



Alleviating abnormal stress on compressed cranial sutures: a potential mechanism for treating and preventing deformational plagiocephaly

Xin Ye^{1†}, Jianfeng Huang^{1†}, Yuanqi Liu², Qianyi Sun¹, Fen Zhang¹, Wei Shen³, Hongda Chen¹, Libin Liu¹, Sumei Chen¹, Ning Yang^{1*}, Ming Yan^{4*} and Zhen Liu^{1*}

Abstract

Background Abnormal stress in cranial sutures is strongly related to deformational plagiocephaly (DP) and is responsible for morphological changes in the skull, facial asymmetry, and abnormal facial tension. To evaluate the effect of biomechanical therapy on cranial sutures of DP we performed in silico analysis of normal skull in the supine position (Model 1), DP in the supine position (Model 2), and DP wearing moulding helmet (Model 3).

Methods By utilizing 3D point cloud data, we generated finite element models (FEMs) and developed 14 cranial sutures. We evaluated the mechanical causes of the continuous progression of moderate to severe DP by comparing the Von Mises Stress (VMS) distributions of 14 cranial sutures between Model 1 and Model 2, and used the same method to compare Model 2 with Model 3 to determine the reasons for the alleviation of DP.

Results When the DP wore a moulding helmet, the VMS on the compressed side of the cranial sutures was reduced, and the skull support site shifted to the contralateral side. DP was associated with abnormal stress accumulation on the compressed side of the cranial sutures. Balancing the forces on both sides of the lambdoid suture, allowing the skull to accept a larger force area and applying stress to the cranial sutures on the uncompressed side may be the mechanism for the prevention and treatment of DP.

Conclusions The asymmetry caused by DP may be associated with abnormal stress accumulation in cranial sutures, and eliminating abnormal stress accumulation in cranial sutures and applying stress to contralateral cranial sutures are key measures of treatment.

[†]Xin Ye and Jianfeng Huang contributed equally to this work.

*Correspondence:

Ning Yang

yn.email@163.com

Ming Yan

yanmingdragon@163.com

Zhen Liu

lzym3798@163.com

Full list of author information is available at the end of the article



Implications for practice

- The force distribution area of the moulding helmet and the degree of head position adjustment may serve as an early indicator for assessing the moulding helmet's efficacy.
- Adding bilateral lambdoid suture support straps to the moulding helmet may be the key to improving the efficacy.
- Our study revealed that the mechanical principles of helmet therapy and osteopathic treatment may support the use of osteopathic treatment as a first-line approach for treating DP.

Keywords Deformational plagiocephaly, Helmet therapy, Osteopathy, Finite element analysis, Cranial sutures

Background

The recommendation issued by the American Academy of Pediatrics in the early 1990s to position infants on their backs during sleep to prevent sudden infant death syndrome (SIDS) has dramatically reduced the number of infant deaths [1]. However, it also markedly increased the incidence rate of positional skull deformation, which rose significantly from approximately 5% to over 46% by the age of 7 months [2]. Abnormal cranial suture stress is the main contributor to DP. Regions of high stress in cranial sutures are of interest, as they determine areas of possible conduction and concern when equipped with a moulding helmet and using osteopathic treatment in DP. The abnormal stress caused by DP can not only lead to facial asymmetry but also affect the motor function of the spine and trunk [3, 4]. Kreuz M [5] and colleagues reported that DP can cause facial asymmetry, and that moulding helmet can improve facial symmetry in infants with DP and correct the associated facial and basal skull asymmetry. Fludder CJ [3] et al. reported significant associations ($P < 0.05$) between cervical flexion and both cervical rotation and DP, but not between lateral flexion and DP. Collett [6] et al. reported that infants with DP presented differences in brain shape, which is consistent with the skull deformity characteristic of this condition, and shape measures were associated with infant development. While asymmetry in brain development exists [7], the asymmetry resulting from DP may be linked to motor developmental delays in infants [8, 9]. At present, the best method for treating DP is to use a moulding helmet for correction [10]. Many studies have confirmed that the moulding helmet does not adversely affect cognitive and intellectual development [11], however, there are certain risks involved in the process of DP treatment [12]. Thus, the key to developing a moulding helmet is to quantify the force application method, site, area, duration, and expected shape.

Biological sutures increase the overall flexibility and fracture toughness of the structure while maintaining the structural integrity provided by the stiffer building blocks [13]. Therefore, finite element analysis (FEA) of the infant skull is used to study the stress distribution, deformation, and stability of the bone structure under external

forces. Remesz R et al. [14] used FEA and reported that the average values of displacement and strain were similar between the two-dimensionally variable and three-dimensionally variable models. Larger ranges and more complex distributions of strain were found in the three-dimensionally variable model. When considering the mechanics of all cranial sutures, taking the true three-dimensional geometry into account for spatial variability and local mechanical response. A semi-brittle material is necessary, the skull is not particularly tough, and it has a large Young's modulus [15]. Experimental testing of goat cranial bone has shown that the geometric features of suture morphology, such as the degree of interdigitation and the length and width of the suture, affect the mechanical response of the material [16].

One potential application of these cranial sutures is in the design of helmets that utilize geometric connections. As such, when wearing a moulding helmet, the structural toughness of cranial sutures is critical for absorbing energy to prevent most loads from being transferred to unilateral sutures [17]. This work expands on these studies by investigating the effects of three models on the mechanical response of cranial sutures in a three-dimensional heterogeneous model derived from 3D point cloud data. Therefore, the goal of this study was to understand the role of cranial sutures in skull mechanics, which may provide insight into the performance of moulding helmets and osteopathic treatment.

Method

3D point cloud data

The 3D scanner was used to scan the skull of the healthy infant to obtain the initial 3D model of the skull. In the Rhinoceros software, we built a head reconstruction program using Grasshopper and entered the 3D point cloud data of the healthy infant's skull into the program to automatically obtain the reconstructed skull surface. The reconstruction process was divided into three steps. First, the data for the triangulated mesh surface were generated according to the 3D point cloud data. Second, we intercepted the section line. Finally, we generated the reconstruction surface according to the section line lofting (Fig. 1).

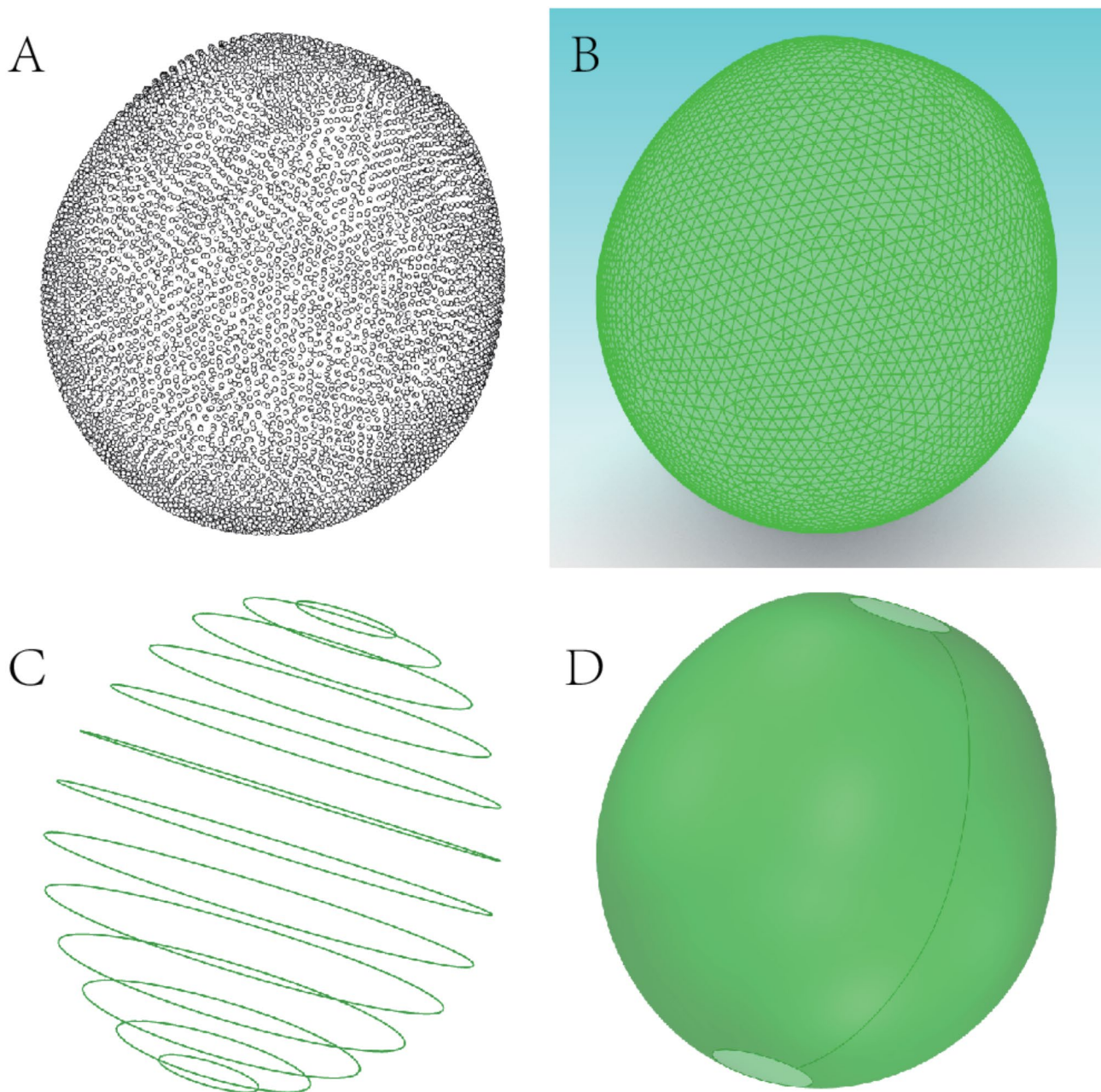


Fig. 1 Processing procedures of 3D point cloud imaging data (A to D)

Moulding helmet model

The inner and outer boundaries of the helmet were determined according to the curved surface of the skull model. A deviation of 2 mm from the curved face of the head was used as the inner boundary of the helmet, whereas a deviation of 17–22 mm was adopted as the outer boundary of the moulding helmet. The contour of the lower boundary of the helmet was determined on the basis of the superficial arch, ears, and occipital bone. We then cut the inner and outer boundary surfaces according to the lower boundary to obtain the basic shape of the helmet.

Finally, the details of the model were processed to create the moulding helmet model (Fig. 2).

Skull model

This study required the construction of a normal skull model and a DP model. These models feature 14 cranial sutures, which are determined according to the layout of the three-dimensional CT reconstruction of the skull model. The 14 cranial sutures included the left lambdoid suture, the right lambdoid suture, the posterior fontanelle, the sagittal suture, the left coronal suture, the right coronal suture, the left squamous suture, the

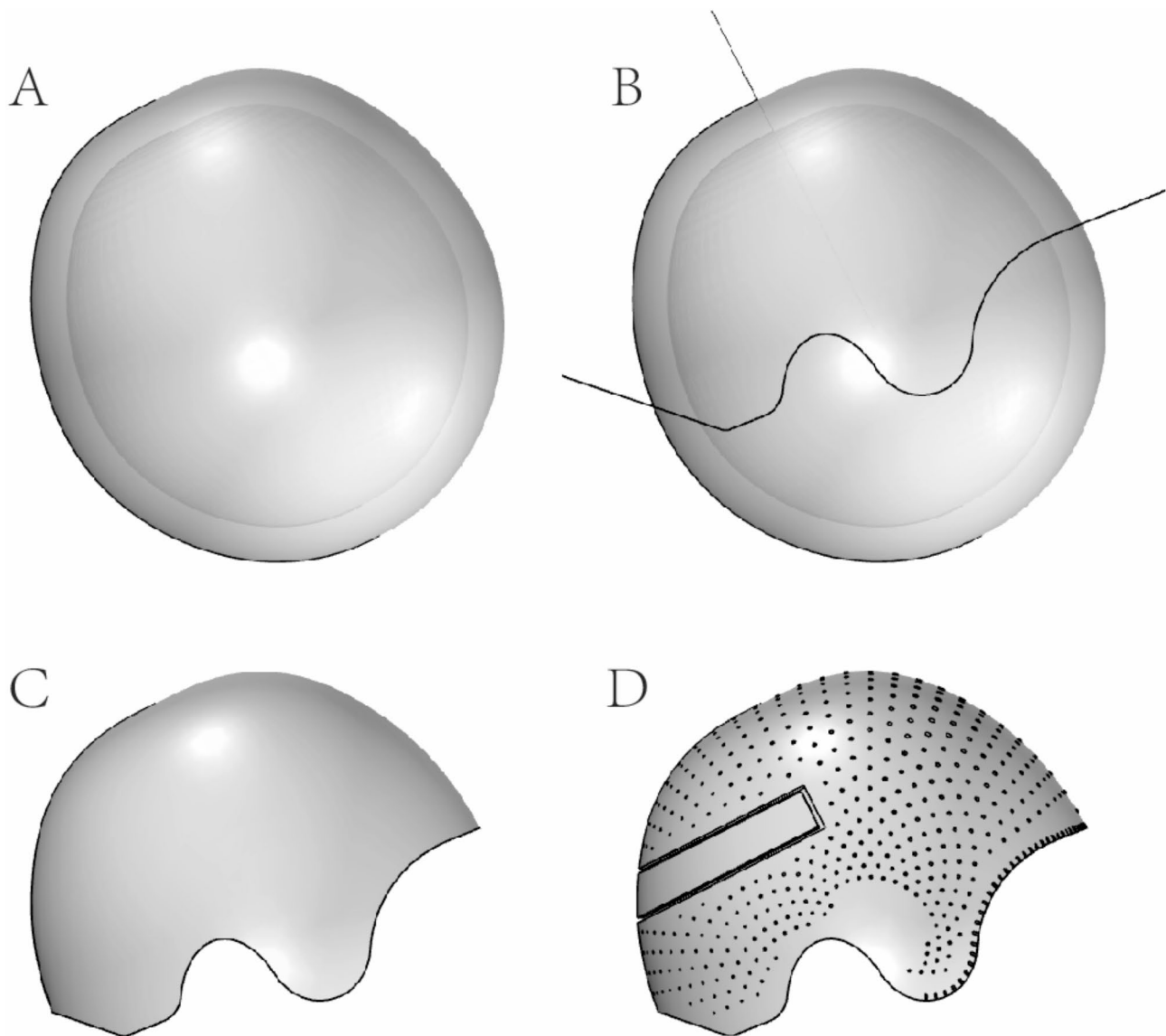


Fig. 2 Production process of the moulding helmet model (A to D)

right squamous suture, the left sphenoid fontanelle, the right sphenoid fontanelle, the left mastoid fontanelle, the right mastoid fontanelle, the anterior fontanelle, and the metopic suture. Then, we constructed the DP model on the basis of the normal skull model, and the entire skull was shifted to the right via the equal offset method. Finally, the 14 cranial sutures followed the curvature of the skull for equal offset (Fig. 3).

Auxiliary model and model assembly

We created a solid model of a rectangular pillow (30 cm × 18 cm × 5 cm) via Rhinoceros software and then imported it as a solid object into ANSYS Workbench 2022. Model 1 consisted of a normal skull model and a pillow model, whereas Model 2 included a DP skull model and a pillow model. Model 1 and Model 2 were

placed on the nonremovable pillow model, the weight of the skull was set to 1.8 kg, and the skull model was allowed to move only in the horizontal direction. Next, Model 3 was created, where a molding helmet model was applied to the DP skull model, allowing the skull to perform only rotational movements around the X (horizontal) axis. At this point, the fixed support of the DP model was placed at the posterior fontanelle, allowing the helmet component to be disregarded during VMS analysis. The material parameters of the three FEMs were set as follows: (1) the thickness of the skull was 3 mm and uniformly distributed across all areas; (2) all the materials exhibited isotropic characteristics; (3) the effects of intracranial pressure, atmospheric pressure, helmet weight, soft tissues, bone modeling, and bone remodeling were considered negligible; (4) the tangential behavior

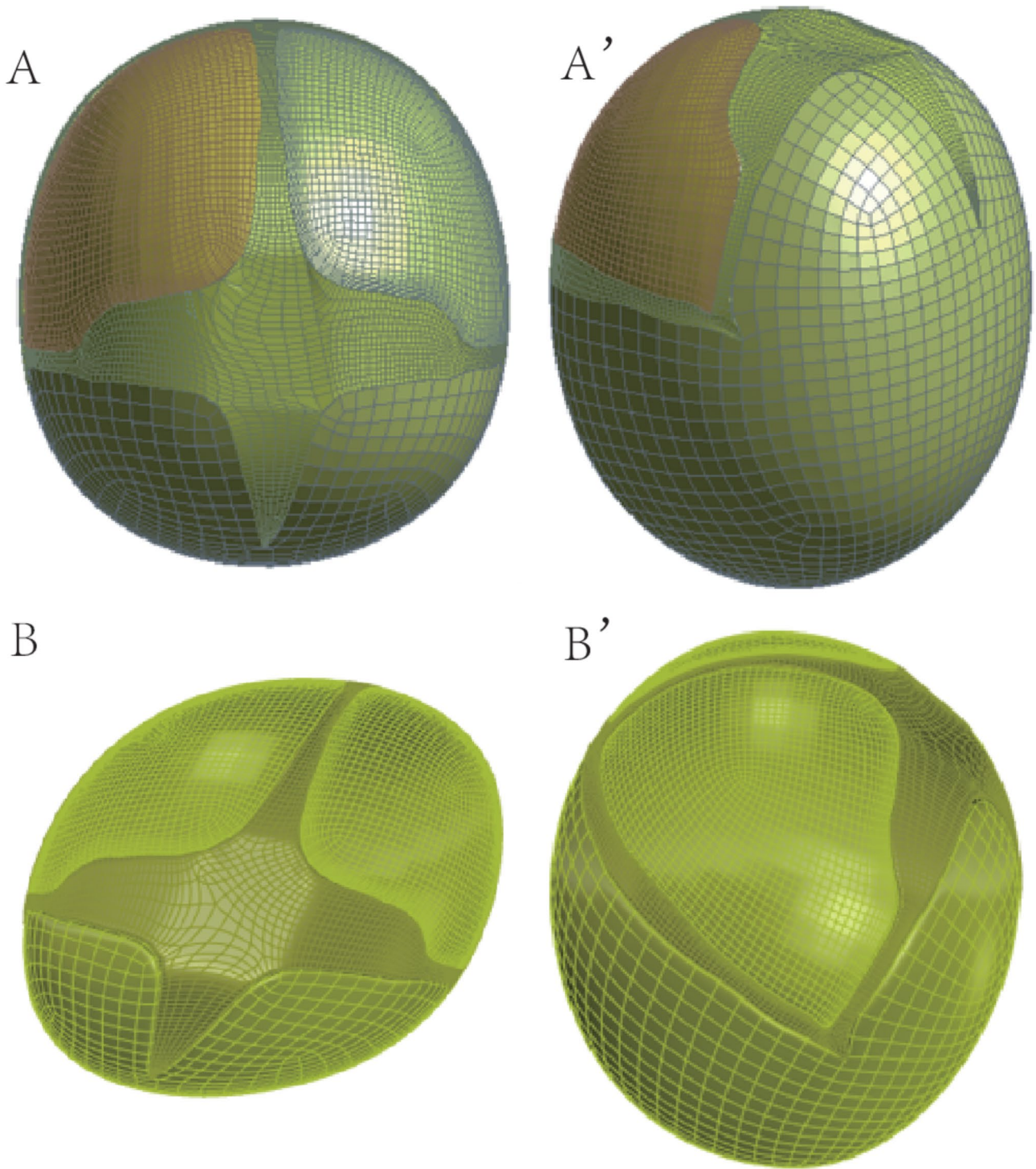


Fig. 3 Normal skull model and DP model. It had 14 cranial sutures. **A** and **A'**: Normal skull model, **B** and **B'**: DP model

Table 1 Young's modulus (MPa) and Poisson's ratio (ν) of the materials used in the study

Component	Young's modulus (MPa)	Poisson's ratio (ν)	References
Moulding helmet	2500	0.3	[18]
Foam pillow	1.2	-0.3	[18]
Cranial sutures	8.11	0.3	[18]

between all the components was treated as frictionless contact, while the normal behavior between all the components was treated as hard contact. (5) To more easily obtain the effect of stress on the cranial suture, the structure of the skull was ignored, and the force values were reduced proportionally to the data of Keshtgar et al. [18]. The mechanical properties of the materials are shown in Table 1. Finally, the data were processed according to the VMS criteria by Keshtgar M [18].

Model validation

To assess the validity of the simulation models, a simplified validation scheme was designed. Since the pressure values only encompass the vertical forces applied to the surfaces of the contact objects, validation is easier. We compared the theoretical pressure exerted by the skull on a pillow or helmet with the pressure values obtained

from the FEMs (Fig. 4). Assuming that the weight of the skull was uniformly distributed over the contact surface, the theoretical average pressure value (TAPA) of the pillow in Model 1 was calculated via the following formula: Pressure (Pa) = [Force (N) / Area (m²)]. Next, the difference between the finite element model average pressure value (FEMAPV) was calculated. Finally, the percentage difference (PD) was obtained as follows: PD=(TAPA - FEMAPV)/TAPA. Similarly, the TAPA, FEMAPV, and PD for Model 2 and Model 3 were also determined. Since the moulding helmet lining had a hemispherical shape, the inner contact radius of the helmet was defined as 6.5 cm. The contact area of the lining can be roughly calculated on the basis of the radius value.

Results

Normal skull in the supine

In the FEA performed for Model 1 in the supine position (Fig. 5A and A'), the maximum average VMS for the cranial sutures was as follows: sagittal suture, mastoid fontanelle, and lambdoid suture. The VMS was uniform in the coronal suture, sphenoid fontanelle, squamous suture and lambdoid suture, whereas it was minimal in the anterior fontanelle and metopic suture (Table 2). The posterior fontanelle was set as a fixed support, resulting in a computer output of 0 Pa. According to observations

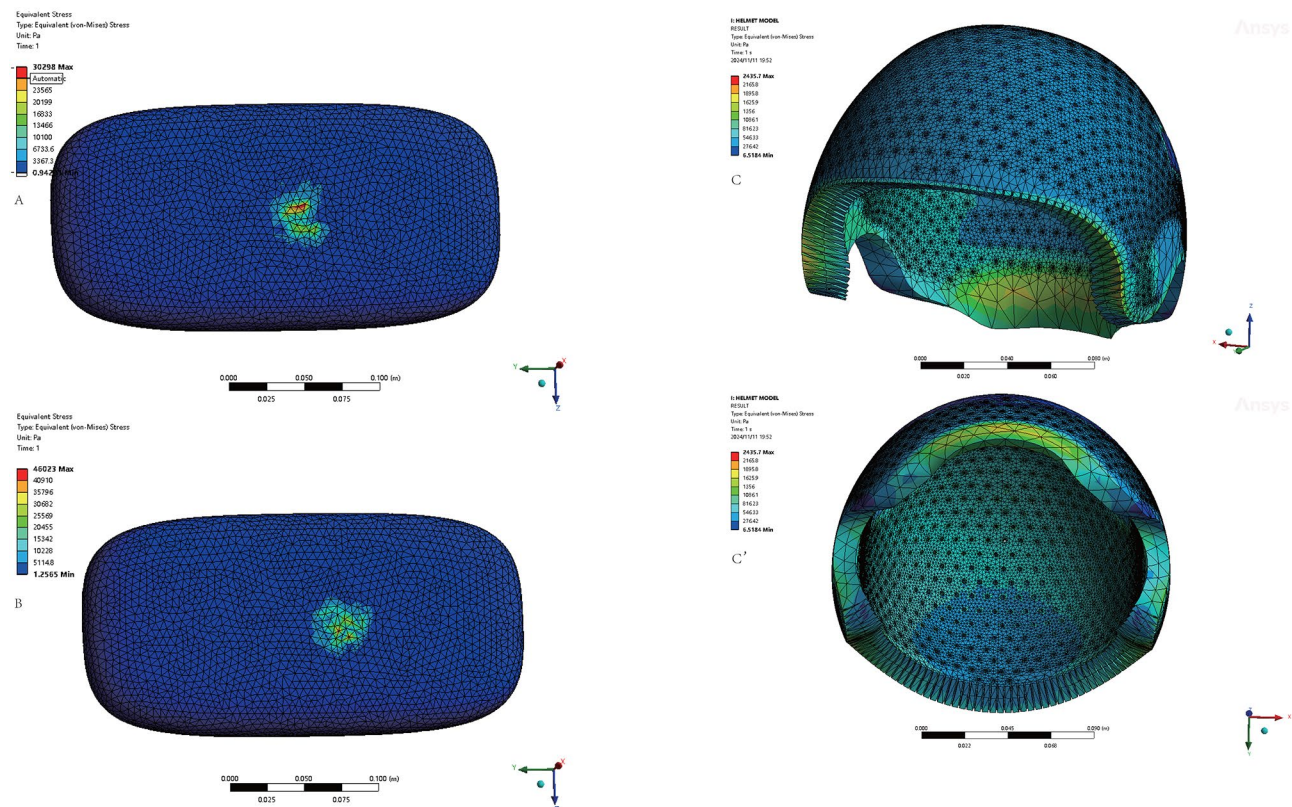


Fig. 4 VMS maps of the Model 1, 2 and 3 contact surfaces. **A:** Model 1; **B:** Model 2; **C** and **C':** Model 3



Fig. 5 The VMS map illustrates cranial sutures in Model 1, 2, and 3. **A** and **A'**: Model 1; **B** and **B'**: Model 2; **C** and **C'**: Model 3

from actual clinical work, the posterior fontanelle is also the main force-bearing site, and its true force value may be greater than that of the sagittal suture and lambdoid suture. However, the closure of the posterior fontanelle typically occurs within 3 months postpartum; therefore, it can be inferred that the true VMS value of the posterior fontanelle is close to that of the lambdoid suture.

DP in the supine

In the FEA performed for Model 2 in the supine position, the maximum average VMS for the cranial sutures was observed in the right sphenoid fontanelle (23,853 Pa). The average VMSs on the right squamous suture, right mastoid fontanelle, right sphenoid fontanelle, frontal suture, anterior fontanelle, and sagittal suture were 11.56 times, 5.56 times, 4.38 times, 2.59 times, 2.55 times, and 1.14 times greater than those in Model 1, respectively (Table 2). Figure 5 (B and B') illustrates that the sleeping position generated by the DP allows for a higher concentration of VMS values on the cranial sutures on the compressed side.

DP with a moulding helmet

In the FEA performed for the DP with a moulding helmet, there was a larger distribution of VMS concentrations across the left cranial sutures with Model 2 (Table 2). The maximum average VMS for the cranial sutures was observed in the left lambdoid suture (24393 Pa). Compared to Model 2, wearing the moulding helmet in the supine position reduced the average VMS at the bilateral lambdoid suture by 50.99%. The average VMS of bilateral lambdoid suture in Model 3 was similar to that in Model 1, which was 15343.15 Pa and 15240.5 Pa, respectively. Additionally, compared with those in Model 2, the

average VMS at the anterior fontanelle, metopic suture, sagittal suture, right coronal suture, right sphenoid fontanelle, right squamous suture, right mastoid fontanelle and right lambdoid suture in Model 3 were reduced by 74.46%, 86.83%, 60.09%, 64.19%, 91.73%, 94.26%, 87.56% and 88.1%, respectively. Figure 5 (C and C') depicts a higher concentration of larger numerically derived VMS values in the left cranial suture of the infant with DP while wearing a moulding helmet.

Predictive performance of FEA

The PDs for Model 1, Model 2, and Model 3 were calculated to be 4.9%, 17.7%, and 12.4%, respectively (Table 3; Fig. 4). In Models 1, 2, and 3, the average VMS standard deviations for all cranial sutures were 4485.01, 5349.04, and 6940.81, respectively.

Discussion

Skull modeling analysis via CAD-CAM-CAE has become a practical and highly predictable approach for clinicians. Our study aimed to provide insight into the mechanical impact of cranial sutures in the DP and DP with a moulding helmet. By using a normal skull as a reference model, the DP model was created via the equal offset method, after which the helmet model was designed on the basis of clinical requirements. Each model component was assembled into FEMs for mechanical analysis, in which the Young's modulus and Poisson's ratio were specified. Although our objective was to gain a deeper understanding of the differences in cranial suture stress among DP patients, normal individuals, and those with DP who use a moulding helmet, we opted for a normal skull as the reference model because of the rapid and dynamic nature of skull development. The duration of orthopedic treatment

Table 2 Minimum, maximum, and average VMS for each cranial suture of .models

cranial suture	Model NO	Number of probes	Minimum VMS (Pa)	Maximum VMS (Pa)	Average VMS (Pa)
1 Anterior fontanelle	Model 1	1455	888.4	7951.2	3849.1
	Model 2	1298	3562.1	22,906	9818.4
	Model 3	1351	764.8	4043.8	2507.4
2 Metopic suture	Model 1	652	0	4502.5	470.2
	Model 2	756	0	10,477	1217.1
	Model 3	673	0	1586.8	166.4
3 Sagittal suture	Model 1	741	0	65,863	15,982
	Model 2	793	1352.5	53,728	18,188
	Model 3	760	0	23,020	7258.1
4 Posterior fontanelle	Model 1	319	0	0	0
	Model 2	334	912	60,027	22,619
	Model 3	317	0	0	0
5 Left Coronal suture	Model 1	1116	97.7	13,157	4041.9
	Model 2	1056	81.8	16,755	7498.4
	Model 3	1058	607.1	12,634	5482.4
6 Right Coronal suture	Model 1	1016	142.9	14,694	4238.4
	Model 2	988	673.8	43,049	7999.4
	Model 3	1046	785.8	6570.3	2864.2
7 Left Sphenoid fontanelle	Model 1	277	0.6	18,107	6474.1
	Model 2	291	0.6	27,072	7222.7
	Model 3	278	0.6	21,012	6768.1
8 Right Sphenoid fontanelle	Model 1	306	2.4	22,974	5953.2
	Model 2	313	4.3	115,280	26,109
	Model 3	307	0.6	9152.9	2156.7
9 Left squamous suture	Model 1	466	183.8	9123.7	4211.5
	Model 2	486	562.6	14,226	7131.2
	Model 3	495	2888.4	20,377	12,438
10 Right squamous suture	Model 1	451	135.9	7593.4	3459.4
	Model 2	416	17,927	65,654	40,011
	Model 3	433	18.5	5203.5	2293.6
11 Left mastoid fontanelle	Model 1	212	1695.6	17,072	8043.7
	Model 2	224	83.8	12,530	3271.7
	Model 3	214	619.6	23,594	8546.3
12 Right mastoid fontanelle	Model 1	264	1167.6	15,034	7677.9
	Model 2	267	787.8	101,880	42,711
	Model 3	268	2119.5	8655.7	5310.4
13 Left lambdoid suture	Model 1	391	0	32,396	14,291
	Model 2	354	0	19,021	9718.6
	Model 3	377	0	92,870	24,393
14 Right lambdoid suture	Model 1	372	0	32,665	16,190
	Model 2	389	787.78	92,956	52,906
	Model 3	381	0	13,087	6293.3

Table 3 TAPA, FEMAPV and PD

Model NO	Contact Area (cm ²)	TAPA (Pa)	FEMAPV (Pa)	PD (%)
Model 1	7.2	24,525	23,305	4.9
Model 2	5.2	33,957	39,989	17.7
Model 3	264.5	667.6	584.4	12.4

with a moulding helmet typically lasts more than three months, and accurately predicting errors related to skull growth and development remains challenging. Therefore, the use of a normal skull as the reference model ensures the consistent temporal alignment of the 3 models and mitigates errors related to skull development. To increase the sensitivity of the cranial suture to stress, we chose to exclude the skull and reduce the stress applied to the cranial suture [18].

The FEMs specifically investigate the localized stress transmission mechanisms at the orthotic helmet-cranial interface. The intracranial pressure system exhibits intrinsic self-equilibration characteristics under static conditions [19]. In typical infant cases, atmospheric pressure acting as a uniformly distributed load demonstrates negligible influence on localized cranial deformation. Although soft tissues with low Young's modulus theoretically enable force dissipation through deformation, the structurally underdeveloped cephalic soft tissue possesses limited deformation capacity to provide effective buffering, thus justifying its exclusion from our computational framework. This static simulation specifically replicates the supine position, given its predominance (>18 h/day) in infant positioning protocols. Under this configuration, gravitational loading constitutes the principal biomechanical determinant, while frictional effects are considered negligible through parametric sensitivity analysis [20]. The current modeling paradigm is specifically designed to elucidate pressure redistribution patterns during the initial helmet intervention phase, rather than predicting long-term morphological evolution. The developmental process of DP is inherently dynamic. To visualize this dynamic transformation process, future research necessitates the integration of advanced modeling techniques with large-scale data training and AI-augmented methodologies. This vision constitutes a critical objective for our forthcoming investigations.

The current computational framework preserves the natural anatomical continuity of cranial sutures without geometrical idealization. Implementing intersection anisotropy (e.g., orthotropic parameters at sagittal-lambdoid suture junctions) in global modeling would necessitate element refinement below 1 mm edge length [17, 21]. Such mesh resolution requirements would incur a threefold increase in computational costs while reaching the validation capacity of clinical CT resolution (typically 0.25–1.0 mm slice thickness) [22]. Furthermore, in this study, there is a need to implement a control-variable approach that removes complex interfering factors (e.g., sweat lubrication, dynamic dislocation) and focuses on the main effect of the support stress provided by the helmet on the distribution of cranial suture pressure. It is in order to be able to clearly observe the VMS environment of the cranial sutures.

A total of 14 cranial sutures' VMS from 3 FEMs were analyzed, revealing various stress patterns. The average VMS of the anterior fontanelle, metopic suture, sagittal suture, right sphenoid fontanelle, right squamous suture, right mastoid fontanelle, and right lambdoid suture in Model 1 was noted to be less than the average VMS in Model 2. The results demonstrate that the asymmetry caused by DP is associated with nonuniform stress in the anterior fontanelle, metopic suture, sagittal suture,

sphenoid fontanelle, squamous suture, mastoid fontanelle, and lambdoid suture. Compared with those in Model 1, the primary stress points on the cranial suture in Model 2 shifted from the posterior fontanelle and the lambdoid suture to the cranial sutures on the compressed side. The human skull consists of irregularly shaped bones with curved surfaces. As the stress experienced by cranial sutures increases, the irregular bones may flatten, leading to cranial sutures directly bearing weight [23]. In cases of DP, the infant's skull may become chronically tilted toward the compressed side of the cranial sutures due to the flattening of that area, potentially resulting in a positional preference [24]. These findings are consistent with the results obtained from palpation of infants with DP, and Fig. 5 shows the VMS map of cranial sutures in the DP while in the supine position, thereby corroborating these results. However, owing to the diversity of forms of DP, this relationship may not be generalized and may be specific to the subject of this study.

Additionally, wearing a moulding helmet for DP can create a more hemilateral distribution of VMS across the 14 cranial sutures, and it increases the VMS on the uncompressed sides of the sphenoid fontanelle, coronal suture, and squamous suture. This suggests that to relieve DP, it is necessary to reduce the VMS on the compressed side of the cranial sutures while increasing the VMS of the sphenoid fontanelle, coronal suture, and squamous suture on the uncompressed side. According to the experimental results presented above, the contact area of Model 3 is 36.7 times greater than that of Model 1 and 50.8 times greater than that of Model 2. A potential explanation for this finding is that wearing a moulding helmet enhances the contact area between the head and the moulding helmet, thereby evenly distributing the weight of the skull across the contact surfaces. Increasing the contact area between the skull and the pillow may help prevent the occurrence of DP. In the supine position, the primary weight-bearing bone of the skull is the occipital bone, and the primary weight-bearing cranial suture is the lambdoid suture. On the basis of the aforementioned results, it is speculated that the early cause of DP results from the uneven forces acting on the lambdoid suture bilaterally. This conclusion may guide us in improving the helmet by designing an auxiliary support strap that provides stable support for the lambdoid suture. When the DP uses a moulding helmet, the position of the cranial sutures on the stressed side changes, which it may be the key to improving the orthopedic effect. Drawing on the theoretical insights gained, enhancing therapeutic efficacy may be achievable through optimizing the helmet design and refining the specifics of osteopathic treatment in DP, thereby expanding the contact area and augmenting the force applied to the uncompressed side of the skull and cranial sutures [10, 25].

This study extends beyond the mechanical analysis of the moulding helmet and provides new insights by conceptualizing the helmet model as extensions of our hands utilized in osteopathic manipulative therapy. Currently, randomized controlled trials have demonstrated the therapeutic effect of osteopathic treatment in DP, which involves applying steady, sustained pressure to the uncompressed side of the skull with both hands [25, 26]. This principle is similar to that of our force application Model 3. Taking the DP model in Fig. 3 as an example, the left occipital and temporal bones, along with the right frontal bone, were frequently used as force application sites. In our clinical work, we teach parents how to massage and gently release tension in the baby's skull during their daily routines, and we inform them of the appropriate amount of force to apply. Similarly, the child's feedback also requires close attention. Osteopathic treatment may be used as a first-line treatment for early DP [27]. This study also paves the way for future research and clinical applications, by incorporating the hands into the model to investigate the underlying principles of osteopathic treatment in DP. Perhaps a new study to employ FEA to simulate the effects of osteopathic treatment on an infant's skull could be conducted in the future.

Limitations of the study

The FEA of the three models requires simplification of the most complex anatomical regions of the skull and cranial sutures. To simplify the skull model, shell elements of uniform thickness were utilized [17]. It requires the simplification of 14 cranial sutures and a reduction in linear material properties. The geometric details of cranial sutures and skull also vary among individuals and depend on genetic and environmental factors. Therefore, there is no single model that can accurately represent all individuals [28]. Our study neglected the intracranial pressure, atmospheric pressure, soft tissue tension, anisotropic behavior of the materials, and friction effects between the materials, all of which could have significantly affected the results, but these factors are manageable in the FEMs.

To present a more intuitive VMS map, the skeletal structure has been omitted, and the stress on the cranial sutures has also been scaled down proportionally. Although the model's data may not accurately reflect real values, it still shows the overall stress trend at the macro level. The moulding helmet is composed of ABS shell material and a nylon 12(PA12) lining. In this study, the helmet was only fixed with ABS material, and the PA12 structure of the inner layer of the helmet, which has a special structure was ignored. The inner PA12 layer of the helmet is relatively soft, which decreases the value of the theoretical overall simulation stress. Since the

connection of the two materials and the inner and outer layers is not considered, an error in the simplified model occurs.

This investigation specifically addresses the predominant etiological paradigms of DP, encompassing prenatal compressive forces and postnatal positional loading, while focusing on established biomechanical hypotheses including cranial suture stress transduction and craniofacial growth dysregulation [29]. Although the craniovertebral junction biomechanics and sacral dural system dynamics exhibit potential pathomechanical correlations with DP progression, their anatomical-functional relationships in infant populations remain contentious [30]. Incorporating atlas (C1) and associated ligamentous structures would necessitate artificial definition of over 10 stress anchoring points and 20+ anisotropic material parameters based on current pediatric cadaveric data scarcity [31, 32]. These structures are influenced by gravitational factors from numerous components, necessitating the artificial setting of certain parameters. However, the excessive inclusion of parameter indicators can severely compromise the validity of the research results. This is why the first cervical and neck soft tissues were not included in the model initially.

Nevertheless, Model 3 still managed to simulate the VMS values of each cranial suture when the moulding helmet was worn. While there are many intrinsic limitations to the FEM of the DP, we believe these studies provide useful insight into biomechanics that would be difficult to ascertain through cadaveric studies.

Conclusions

We utilized FEA to evaluate 14 cranial sutures in 3 FEMs, which included the normal skull in the supine position, the DP in the supine position and the DP with a moulding helmet. During the development of DP, FEA revealed significant VMS changes in the right squamous suture, right mastoid fontanelle, right sphenoid fontanelle, frontal suture, anterior fontanelle, and sagittal suture. This finding suggests that facial asymmetry resulting from DP may be related to stress abnormalities in these cranial sutures. The uneven force on the lambdoid suture on both sides may be a contributing factor to DP. Expanding the stress distribution on the skull and balancing the forces on the lambdoid suture may help prevent DP. When a moulding helmet is worn, stress is transferred to the contralateral cranial suture, thus reducing stress on the originally compressed cranial suture and allowing space to grow. While FEA of a normal skull, DP and DP with a moulding helmet require oversimplification of a complex anatomical region, this study provides biomechanical insight into 14 cranial sutures, which reveal the development and healing process of DP.

Abbreviations

DP	Deformational plagiocephaly
FEA	Finite element analysis
FEMs	Finite element models
VMS	Von Mises stress
TAPA	Theoretical Average Pressure Value
FEMAPV	Finite Element Model Average Pressure Value
PD	Percentage Difference
PA12	Nylon 12

Supplementary Information

The online version contains supplementary material available at <https://doi.org/10.1186/s13052-025-01955-3>.

Supplementary Material 1

Acknowledgements

We thank Dr. Haiyan Mao for English language editing and pictures editing.

Author contributions

Conceptualization, ZL, NY, MY and XY; Methodology, ZL, NY, JFH and XY; Software, XY, WS and LYQ; Data Curation, XY, JFH, QYS, and FZ; Writing – Review & Editing, XY, HDC, SMC and LBL; Project Administration, ZL, XY, NY, and JFH; Funding Acquisition, ZL, MY. Among the three co-corresponding authors, Zhen Liu has been designated as the primary contributor.

Funding

This research was supported by the Science and Technology Project in Key Areas of Foshan (Grant No. 2020001005717), the Guangzhou Clinical Characteristic Technology Project (Grant No.2023 C-TS16), the 2023 Basic Research Plan Project (2023 Guangzhou School [institute] Enterprise joint funding topic (Grant No.557), the Foshan Digital Intelligent Manufacturing Rehabilitation Aids Innovation Engineering Technology Research Centre (Grant No. 011102).

Data availability

The data presented in this study are available upon request from the corresponding author.

Declarations

Ethics approval and consent to participate

The study was approved by the Research Ethics Board of The Third Affiliated Hospital of Guangzhou Medical University, China (chiCTR-OIC-17013130). Ethics approval and consent to participate Ethical approval was not necessary as this was a computerized analysis experiment.

Consent for publication

Written informed consent for publication was obtained.

Competing interests

The authors declare that they have no conflicts of interest.

Author details

¹Department of Rehabilitation Medicine, Guangdong Provincial Key Laboratory of Major Obstetric Diseases, Guangdong Provincial Clinical Research Center for Obstetrics and Gynecology, The Third Affiliated Hospital, Guangzhou Medical University, Guangzhou, China

²Department of Zhuhai Keyu Biological Engineering, Guangzhou, China

³Department of Ameba Engineering Structure Optimization Research Institute, Nanjing, China

⁴Department of gynecology, The First People's Hospital of Foshan, Foshan, China

Received: 21 November 2024 / Accepted: 27 March 2025

Published online: 16 April 2025

References

1. Dwyer T, et al. Prospective cohort study of prone sleeping position and sudden infant death syndrome. *Lancet* (London England). 1991;337(8752):1244–7. [https://doi.org/10.1016/0140-6736\(91\)92917-q](https://doi.org/10.1016/0140-6736(91)92917-q).
2. Santiago GS, et al. Positional Plagiocephaly and craniosynostosis. *Pediatr Ann*. 2023;52(1). <https://doi.org/10.3928/19382359-20221114-03>. p. e10-e17.
3. Fludder CJ, Keil BG. Deformational Plagiocephaly and reduced cervical range of motion: A pediatric case series in a chiropractic clinic. *Altern Ther Health Med*. 2021;27(6):26–32.
4. Naros A, et al. Three-Dimensional quantification of facial asymmetry in children with positional cranial deformity. *Plast Reconstr Surg*. 2021;148(6):1321–31. <https://doi.org/10.1097/PRS.0000000000008564>.
5. Kreutz M, et al. Facial asymmetry correction with moulded helmet therapy in infants with deformational skull base plagiocephaly. *Surgery*. 2018;46(1):28–34. <https://doi.org/10.1016/j.jcms.2017.10.013>. *Journal of cranio-maxillo-facial surgery: official publication of the European Association for Cranio-Maxillo-Facial*.
6. Collett BR, et al. Brain volume and shape in infants with deformational Plagiocephaly. *Child's nervous system: ChNS. Official J Int Soc Pediatr Neurosurg*. 2012;28(7):1083–90. <https://doi.org/10.1007/s00381-012-1731-y>.
7. Kurth F, et al. Large-scale analysis of structural brain asymmetries during neurodevelopment: associations with age and sex in 4265 children and adolescents. *Hum Brain Mapp*. 2024;45(11):e26754. <https://doi.org/10.1002/hbm.26754>.
8. Knight SJ, et al. Early neurodevelopment in infants with deformational Plagiocephaly. *J Craniofac Surg*. 2013;24(4):1225–8. <https://doi.org/10.1097/SCS.0b013e318299777e>.
9. Collett BR et al. Do infant motor skills mediate the association between positional Plagiocephaly/Brachycephaly and cognition in School-Aged children?? *Physical therapy*. 2021. 101(2). <https://doi.org/10.1093/ptj/pzaa214>
10. Kropla F, et al. Development of an individual helmet orthosis for infants based on a 3D scan. *3D Print Med*. 2023;9(1):22. <https://doi.org/10.1186/s41205-023-00187-7>.
11. Park KE, et al. Neurocognitive outcomes in deformational Plagiocephaly: is there an association between morphologic severity and results?? *Plast Reconstr Surg*. 2023;152(3):e488–98. <https://doi.org/10.1097/PRS.00000000000010330>.
12. Gump WC, Mutchnick IS, Moriarty TM. Complications associated with molding helmet therapy for positional Plagiocephaly: a review. *NeuroSurg Focus*. 2013;35(4):E3. <https://doi.org/10.3171/2013.5.FOCUS.13224>.
13. Fratzl P, et al. The mechanics of tessellations - bioinspired strategies for fracture resistance. *Chem Soc Rev*. 2016;45(2):252–67. <https://doi.org/10.1039/c5cs00598a>.
14. Remesz R et al. Cranial suture morphometry and mechanical response to loading: 2D vs. 3D assumptions and characterization. *Biomechanics and modeling in mechanobiology*, 2022;21(4):1251–65. <https://doi.org/10.1007/s10237-022-01588-z>
15. Rho JY, Ashman RB, Turner CH. Young's modulus of trabecular and cortical bone material: ultrasonic and microtensile measurements. *J Biomech*. 1993;26(2):111–9. [https://doi.org/10.1016/0021-9290\(93\)90042-d](https://doi.org/10.1016/0021-9290(93)90042-d).
16. Jaslow CR. Mechanical properties of cranial sutures. *J Biomech*. 1990;23(4). [https://doi.org/10.1016/0021-9290\(90\)90059-c](https://doi.org/10.1016/0021-9290(90)90059-c). 313–21.
17. Gibbons MM, Chen DA. Bio-Inspired sutures: using finite element analysis to parameterize the mechanical response of dovetail sutures in simulated bending of a curved structure. *Biomimetics* (Basel Switzerland). 2022;7(2). <https://doi.org/10.3390/biomimetics7020082>.
18. Keshtgar M. Evaluating the Effectiveness of Cranial Molding for Treatment of Positional Plagiocephaly Using Finite Element Analysis. 2015.
19. Bothwell SW, Janigro D, Patabendige A. Cerebrospinal fluid dynamics and intracranial pressure elevation in neurological diseases. *Fluids Barriers CNS*. 2019;16(1):9. <https://doi.org/10.1186/s12987-019-0129-6>.
20. Stark NE, et al. The influence of headform friction and inertial properties on oblique impact helmet testing. *Ann Biomed Eng*. 2024;52(10):2803–11. <https://doi.org/10.1007/s10439-024-03460-w>.
21. Gibbons MM, Chen DA. Bio-Inspired sutures: simulating the role of suture placement in the mechanical response of interlocking structures. *Biomimetics* (Basel Switzerland). 2023;8(7). <https://doi.org/10.3390/biomimetics8070515>.
22. Pham N, et al. High-Resolution CT imaging of the Temporal bone: A cadaveric specimen study. *Journal of neurological surgery. Part B. Skull Base*. 2022;83(5):470–5. <https://doi.org/10.1055/s-0041-1741006>.

23. Smartt MJ, et al. Analysis of differences in the cranial base and facial skeleton of patients with lambdoid synostosis and deformational Plagiocephaly. *Plast Reconstr Surg*. 2011;127(1):303–12. <https://doi.org/10.1097/PRS.0b013e3181f95cd8>.
24. van Vlimmeren LA, et al. Effect of pediatric physical therapy on deformational Plagiocephaly in children with positional preference: a randomized controlled trial. *Arch Pediatr Adolesc Med*. 2008;162(8):712–8. <https://doi.org/10.1001/archpedi.162.8.712>.
25. Bagagiolo D, et al. A randomized controlled trial of osteopathic manipulative therapy to reduce cranial asymmetries in young infants with nonsynostotic Plagiocephaly. *Am J Perinatol*. 2022;39:01. <https://doi.org/10.1055/s-0042-1758723>.
26. Pastor-Pons I, et al. Efficacy of pediatric integrative manual therapy in positional Plagiocephaly: a randomized controlled trial. *Ital J Pediatr*. 2021;47(1):132. <https://doi.org/10.1186/s13052-021-01079-4>.
27. Panza R, et al. Positional Plagiocephaly: results of the osteopathic treatment of 424 infants. An observational retrospective cohort study. *Ital J Pediatr*. 2024;50(1):166. <https://doi.org/10.1186/s13052-024-01729-3>.
28. Henderson JH, et al. Age-dependent properties and quasi-static strain in the rat sagittal suture. *J Biomech*. 2005;38(11):2294–301. <https://doi.org/10.1016/j.jbiomech.2004.07.037>.
29. Wang MM et al. The 27 facial sutures: timing and clinical consequences of closure. *Plastic and reconstructive surgery*, 2022;149(3):701–20. <https://doi.org/10.1097/PRS.0000000000008816>
30. Carreiro J. Pediatric manual medicine: an osteopathic approach. 2009.
31. Salavcová L, et al. Pediatric atlas anatomy and its implications for fracture treatment: an anatomical and radiological study. *Neurocirugia (English Edition)*. 2024;35(4):186–95. <https://doi.org/10.1016/j.neucie.2024.01.001>.
32. Song E, et al. Recent advances in microsystem approaches for mechanical characterization of soft biological tissues. *Microsystems Nanoengineering*. 2022;8:77. <https://doi.org/10.1038/s41378-022-00412-z>.

Publisher's note

Springer Nature remains neutral with regard to jurisdictional claims in published maps and institutional affiliations.